Research Article Vol. 4, No. 6 / 15 June 2021 / OSA Continuum 1889

Comparison of two low-noise CEO frequency stabilization methods for an all-PM Yb:fiber NALM oscillator

SARPER SALMAN,[1,2,3,*] YUXUAN MA,[1] KUTAN GÜREL,[4] STÉPHANE SCHILT,[4] CHEN LI,[1] PHILIP PFÄFFLEIN,[1,2,3] CHRISTOPH MAHNKE,[1] JAKOB FELLINGER,[5] STEFAN DROSTE,[6] ALINE S. MAYER,[5] OLIVER H. HECKL,[5] THOMAS SÜDMEYER,[4] CHRISTOPH M. HEYL,[1,2,3] AND INGMAR HARTL[1]

[1]*Deutsches Elektronen-Synchrotron DESY, Notkestraße 85, 22607 Hamburg, Germany*
[2]*Helmholtz-Institute Jena, Fröbelstieg 3, 07743 Jena, Germany*
[3]*GSI Helmholtzzentrum für Schwerionenforschung GmbH Planckstraße 1, 64291 Darmstadt, Germany*
[4]*Laboratoire Temps-Fréquence, Université de Neuchâtel, CH-2000 Neuchâtel, Switzerland*
[5]*University of Vienna, Faculty of Physics, Faculty Center for Nano Structure Research, Christian Doppler Laboratory for Mid-IR Spectroscopy and Semiconductor Optics, 1090 Vienna, Austria*
[6]*SLAC National Accelerator Laboratory, 2575 Sand Hill Rd, Menlo Park, CA 94025, USA*
[*]*sarper.salman@desy.de*

Abstract: We present a comparison of two low-noise carrier-envelope offset (CEO) frequency stabilization methods studied using an ytterbium (Yb) fiber laser oscillator based on a nonlinear amplifying loop mirror. We first investigate the phase locking performance achieved with cross-gain modulation (XGM) via injection of an auxiliary low-power continuous-wave (CW) laser into the fiber gain medium. Amplification of the injected CW laser light cross-modulates the gain of the oscillator, resulting in an intra-cavity power modulation, thus providing control of the CEO frequency. The XGM method is then compared with the conventional pump-current modulation scheme. Both stabilization methods provide similar locking performances with sub-200-mrad of integrated residual carrier-envelope-phase (CEP) noise (10 Hz to 1 MHz), suitable for high-resolution comb spectroscopy applications.

1. Introduction

Over the last two decades we have witnessed a rapid advance in optical frequency comb technology. Due to their evenly spaced ultra-narrow comb-lines and their extremely high phase-coherence, optical frequency combs quickly found applications in many fields. Although originally developed for providing a direct frequency link between the optical and radio-frequency (RF) domains as basis for optical atomic clocks [1], today applications include the calibration of astronomical spectrographs, trace gas sensing, precision time/frequency transfer applications, molecular fingerprinting, coherent control in field-depending processes as well as molecular spectroscopy [2–5]. Passively mode-locked laser oscillators are typically used for generating optical frequency combs. A widely used mode-locking method employs nonlinear polarization evolution (NPE), partially combined with saturable absorbers (SAs) [6–11]. More recently, oscillators employing nonlinear amplifying loop mirrors for mode-locking have emerged as promising alternative [12–16].

Achieving a fully-stabilized optical frequency comb requires the stabilization of two degrees of freedom such as the repetition rate (f_{rep}) and the carrier-envelope offset frequency (f_{ceo}) [17].

#424340 https://doi.org/10.1364/OSAC.424340
Journal © 2021 Received 5 Mar 2021; revised 18 May 2021; accepted 20 May 2021; published 15 Jun 2021

OSA CONTINUUM

The repetition rate can be stabilized, for instance, to a low-noise radio-frequency synthesizer via a feedback loop actuating on the end mirror of the laser oscillator. Stabilization of f_{ceo} is traditionally achieved by controlling the pump diode power of the laser after detecting the CEO beat via f-to-2f interferometry [17]. This method is relatively simple and easy to implement. However, since the feedback bandwidth of this traditional pump power modulation method is limited by the gain lifetime of the active medium as well as by cavity dynamics [18], alternative methods have been demonstrated to overcome these limitations [19–21]. Lee et al. have shown that relatively high f_{ceo}-locking bandwidths can be achieved via cavity loss modulation using a graphene-based electro-optical loss modulator [19]. In contrast to pump power modulation, cavity loss modulation creates direct changes in the circulating intra-cavity power, preventing bandwidth limitations due to the gain lifetime, translating the limitation to the bandwidth of the electro-optical modulator (EOM). However, this method brings along increased complexity and cost and the system still requires a slow feedback to the pump power of the oscillator for long-term operation. Similar to the EOM technique, Pronin et al. demonstrated that the CEO frequency can be stabilized using an intra-cavity acousto-optical modulator (AOM) as a loss modulator, reaching a residual integrated phase noise of 180 mrad (in-loop measurement in the frequency band of 1 Hz – 500 kHz) [22]. A different approach to implement an intra-cavity loss modulator makes use of an opto-optical modulator (OOM) achieved by optically-modulating a semiconductor saturable absorber mirror (SESAM) in diode-pumped solid-state mode-locked lasers (DPSSLs). Hoffmann et al. [21] demonstrated less than 65 mrad residual integrated phase noise (1 Hz – 100 kHz) and Hakobyan et al. [23] measured 430 mrad residual integrated phase noise (10 Hz – 1 MHz) by using a SESAM as a fast OOM in a GHz repetition rate Yb:CALGO DPSSL.

A more recent approach for f_{ceo} stabilization relies on modulating the laser gain medium using an auxiliary laser. Employing this scheme for an Er:Yb:glass diode-pumped solid-state laser (SESAM mode-locked, 100 MHz repetition rate), Karlen et al. [24] demonstrated 120 mrad integrated phase noise (1 Hz to 1 MHz). Gürel et al. [25] employed a similar cross-gain modulation (XGM) method for f_{ceo} stabilization of a fiber laser (NPE mode-locked, 125 MHz repetition rate) reaching a 400-kHz modulation bandwidth using a low-power (< 1 mW) auxiliary CW laser, surpassing the locking performance achieved using the pump-modulation method. Andrade et al. [26] demonstrated 1.4-radian integrated phase noise (100 Hz to 500 kHz) following a similar approach but employing a thin-disk laser (Kerr-lens mode-locked, 32.5 MHz repetition rate) and using part of the laser's output as CEP modulation source. Modulating the laser gain using an auxiliary laser was found to be advantageous in order to overcome lifetime-induced bandwidth limitations [24,25] as well as the challenge of modulating high-power pump-diodes with large bandwidth [27].

Here, we implement CEO stabilization via XGM in an environmentally-stable ytterbium -based nonlinear amplifying loop mirror (NALM) oscillator. We compare the XGM method with the traditional pump modulation approach. With both methods, sub-200-mrad integrated phase noise (10 Hz to 1 MHz) was achieved, enabling high-coherence frequency comb applications.

2. Experimental setup

The oscillator employed in this work is schematically shown in Fig. 1. Mode-locking is achieved using the NALM-based mode-locking method, i.e. the saturable absorber-like reflectance properties of a nonlinear fiber loop caused by the interference of two counter-propagating pulses in a 50:50 coupler [28].

The fiber loop is formed by connecting two outputs of the 50:50 2×2 coupler (CPL1). Inside the loop there is an Yb-doped fiber, a wavelength division multiplexer (WDM) and a non-reciprocal phase shifter comprised of two polarization beam splitters, two Faraday rotators and a wave plate. The phase shifter is used to assist mode-locking and self-starting of the

OSA CONTINUUM

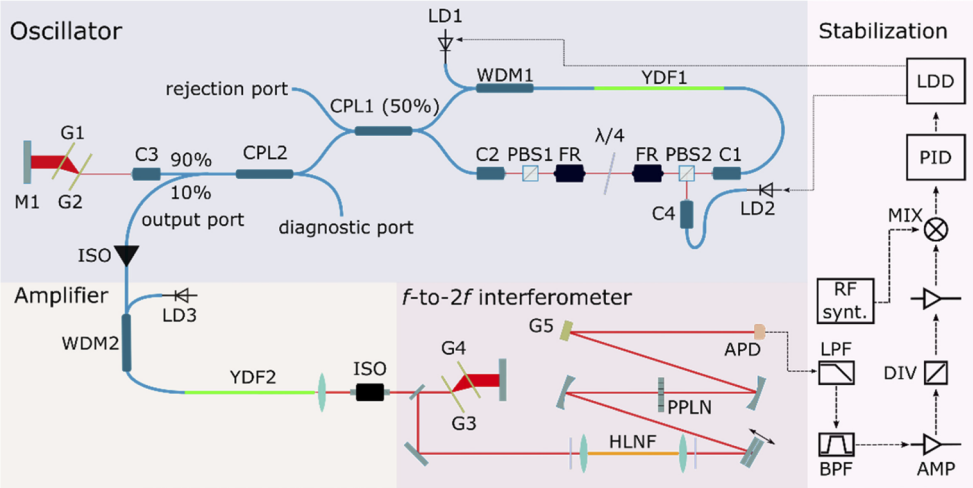

Fig. 1. Experimental setup (LD: laser diode, FR: faraday rotator, WDM: wavelength division multiplexer, CPL: coupler, YDF: Ytterbium doped fiber, C: fiber coupled collimator, PBS: polarizing beam splitter, G: grating, ISO: isolator, HLNF: highly nonlinear fiber, PPLN: periodically-poled lithium niobate crystal, APD: avalanche photodiode, PID: proportional-integral-derivative servo controller, LDD: laser diode driver, RF synt.: RF synthesizer, LPF: low pass filter, BPF: band pass filter, AMP: RF amplifier, DIV: frequency divider, MIX: frequency mixer, blue: passive fiber, green: active fiber, red: free space beam).

oscillator [29]. On the other side of the CPL1 is a linear arm which consists of a grating pair, a 90:10 coupler and an end mirror. The gain medium is a 55-cm-long PM Yb-doped fiber (Nufern PM-YSF-HI-HP – YDF1). It is pumped by a 976-nm pump diode (LD1) coupled via a 980/1030 nm wavelength division multiplexer (WDM1). One end of the coupler (rejection port) is used for diagnostics and the other end is spliced to the linear arm. An intra-cavity transmission grating pair (1000 lines/mm – G1, G2) is placed in the linear arm and adjusted to approximately compensate the cavity dispersion of the oscillator, which in this work was operated with a net cavity dispersion of about -0.019 ps^2 (estimated via a precise measurement of the fiber length and grating separation). The 10% port of a 2×2 fiber coupler (PM, fast-axis-blocked – CPL2) with a 90:10 splitting ratio in the linear arm serves as an output coupler.

The output power of the oscillator from the output coupler and the rejection port is 4.5-mW and 2.6 mW, respectively. The oscillator operates at a repetition rate of 65 MHz emitting a spectrum with a 17-nm full-width at half-maximum (FWHM) bandwidth as depicted in Fig. 2(a). The corresponding pulse duration after compression is 110 fs, measured via second harmonic generation frequency-resolved optical gating (SHG FROG). Temporal pulse profile as well as measured and reconstructed SHG FROG traces are shown in Fig. 2(b) and Fig. 2(c, d), respectively.

For CEO-stabilization using the XGM method, light from an auxiliary laser diode is injected into the oscillator via the unused port of a PBS (PBS2). The light of the auxiliary laser diode (LD2) passes the active fiber in the unused fast axis but gets blocked by the coupler (fast-axis-blocked) located in the linear arm (CPL2). This way, it is possible to act on the gain dynamics in the gain fiber while keeping the amplifier and f-to-2f interferometer unaffected by the auxiliary laser wavelength. Two different auxiliary laser diodes (continuous wave operation) with center wavelengths of 1025-nm (Lumics - LU1025M300) and 1080-nm (Lumics - LU1080M300), respectively, were tested and the maximum injected power level was measured to be 4 mW for both diodes.

OSA CONTINUUM

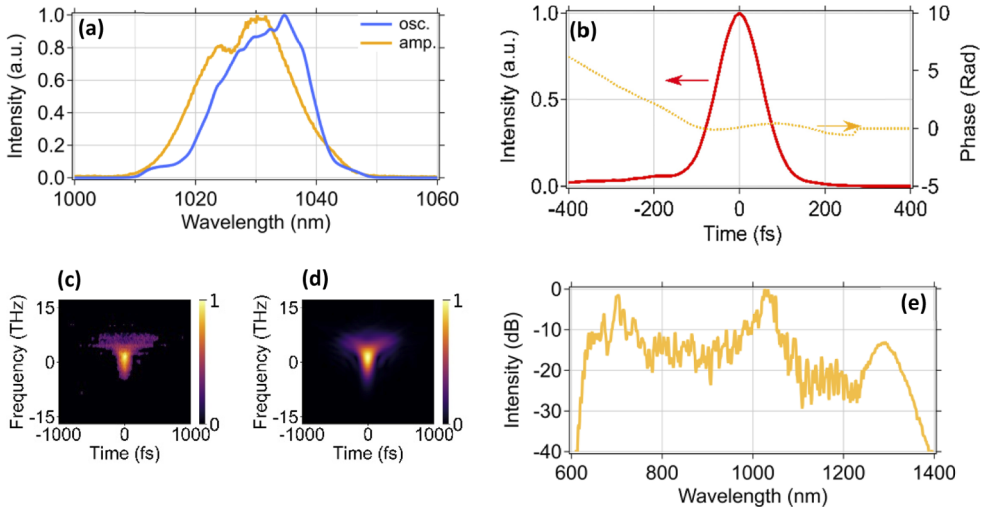

Fig. 2. (a) Optical spectra from the Yb:fiber NALM oscillator measured at the output port (blue) and after the Yb amplifier (orange). (b) Retrieved temporal intensity and phase. (c) Measured and (d) Reconstructed SHG FROG traces. (e) Octave-spanning supercontinuum spectrum generated in a highly-nonlinear fiber.

In order to achieve an octave-spanning spectrum, which is needed for f_{ceo} beat detection using an f-to-$2f$ interferometer, an Yb-fiber amplifier is used to enhance the peak power of the oscillator. The fiber amplifier consists of a 90-cm PM Yb-doped gain fiber (Nufern PM-YSF-HI-HP – YDF2) pumped by a 976-nm pump diode (LD3) with 600 mW of output power and a 980/1030-nm WDM (WDM2). A transmission grating (1000 lines/mm – G3, G4) compressor is placed after the amplifier while a free-space isolator is protecting the system from back-reflections. The output power of the amplifier is 280 mW, the measured pulse duration is 108 fs. The amplified light is then injected into a 16-cm highly-nonlinear suspended-core fiber [30] with a 72% coupling efficiency for spectral broadening. The emitted octave-spanning spectrum is shown in Fig. 2(e).

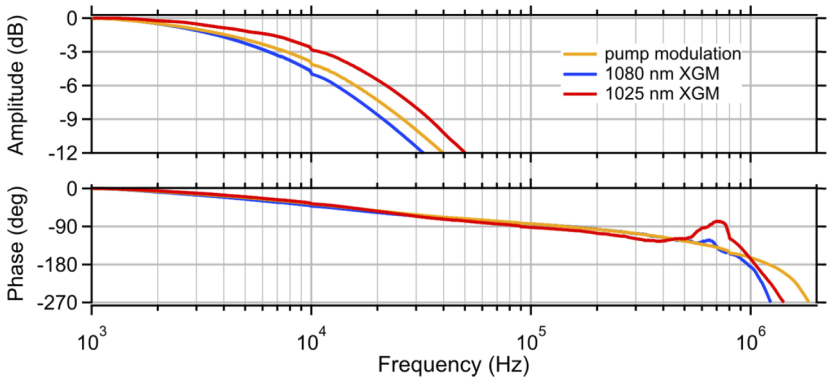

Fig. 3. Transfer function of the diode driver to the Yb:NALM oscillator output power for pump current modulation (orange) and XGM (blue for the 1080-nm auxiliary laser diode current modulation and red for the 1025-nm auxiliary laser diode current modulation). All curves are offset to 0 at 1 kHz.

OSA CONTINUUM

We use a collinear f-to-$2f$ interferometer to generate the f_{ceo} beat signal. In the interferometer, the longer wavelength part of the supercontinuum (1300 nm) is frequency-doubled in a periodically-poled lithium niobate (PPLN) crystal and then overlapped spatially with the shorter wavelength part (650 nm) on an avalanche photodiode (APD). Temporal overlap is achieved by employing reflection by two closely spaced mirror surfaces, reflecting short and long wavelengths, respectively. For f_{ceo} detection, the output of the f-to-$2f$ interferometer is optically-filtered using a grating before impinging onto the APD. The detected f_{ceo} beat with 27-dB signal-to-noise ratio (SNR) in 100-kHz resolution bandwidth in free-running mode is depicted in Fig. 4(a).

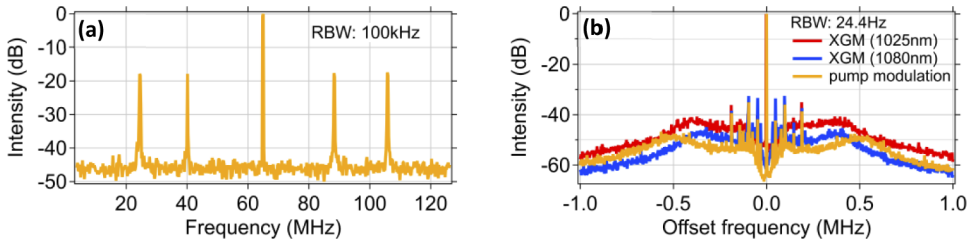

Fig. 4. (a) RF spectrum of the free-running CEO beat signals with 27-dB SNR in 100-kHz resolution bandwidth (RBW), centered around the fundamental repetition rate of the oscillator (65 MHz). (b) RF spectrum of the stabilized CEO beat signal for both locking methods with 24.4-Hz resolution bandwidth (RBW).

3. Experiments and results

For f_{ceo} stabilization, the bandwidth of the feedback loop used for locking plays a crucial role. To characterize the achievable bandwidth for the two locking methods discussed in this paper, we performed transfer function measurements from the laser diode driver current to the output power of the oscillator. We have also performed transfer function measurements from laser diode driver current to the output power of the laser diode to verify that the laser diode/diode driver does not limit the achieved bandwidth. For both auxiliary laser diodes and the pump diode of the oscillator we measure a bandwidth exceeding 1 MHz (for both ± 3 dB in amplitude and ± 90° phase change), confirming that the laser diode and driver does not set a limit in our experiment.

The current of the laser diodes (pump diode for the pump modulation method and auxiliary diodes for the XGM method) is modulated using a vector source analyzer (HP 89441A) while recording the output power of the oscillator using a photodiode. The measured transfer functions are shown in Fig. 3. For both pump-modulation and XGM methods, similar bandwidths are achieved, reaching about 7–10 kHz (3-dB amplitude) or 100 kHz (for 90° phase detuning). A proportional-integral-derivative (PID) loop filter is employed later on for achieving larger f_{ceo} locking bandwidths.

The radio-frequency (RF) output of the APD is filtered, amplified and pre-scaled by a factor of 4 (300 MHz / 4) using RF components. The f_{ceo} beat signal is then phase-compared to a low-noise RF synthesizer (Rohde & Schwarz SML01) using a digital phase detector in order to generate a phase error signal for feedback control. The error signal is fed to a fast PID loop filter connected to a current modulator which drives either the 976-nm pump diode of the oscillator for pump modulation or one of the auxiliary diodes (1025 nm or 1080 nm) for XGM. The same current modulator was used for both stabilization methods. The RF spectrum of the stabilized f_{ceo} beat is depicted in Fig. 4(b) for both locking methods.

The residual f_{ceo} phase noise is characterized for both locking methods using a signal source analyzer (Agilent E5052B). The power spectral density of the residual phase noise of the stabilized f_{ceo} beat is shown in Fig. 5 for pump modulation and XGM methods including a loosely locked

OSA CONTINUUM

scenario. A Thorlabs Pro8000 current driver is used for the loose lock with servo-bandwidth of approximately 15 kHz.

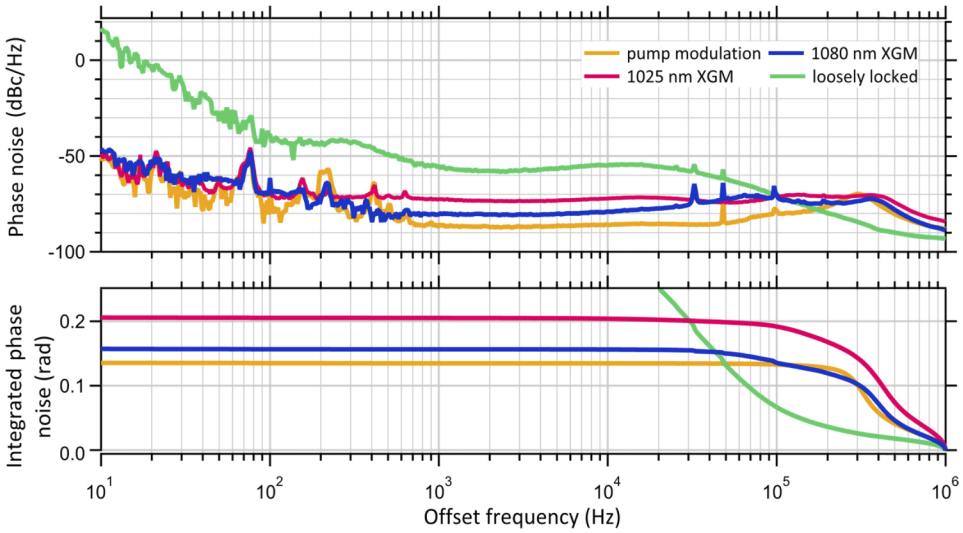

Fig. 5. Single sideband phase noise power spectral density of the stabilized CEO beat signal for both stabilization methods (red, yellow and blue lines) including a loosely locked scenario (green line) along with integrated phase noise from 10 Hz to 1 MHz.

For both f_{ceo} stabilization methods, a locking bandwidth of about 350 kHz is obtained. We achieve in-loop integrated f_{ceo} phase noise (10 Hz to 1 MHz) of 135 mrad, 157 mrad and 206 mrad for pump-modulation, XGM via a 1080-nm auxiliary laser diode and XGM via a 1025-nm auxiliary laser diode, respectively. We attribute the difference between XGM pumped at 1080 nm and 1025 nm to different gain dynamics caused by pumping within and outside the Yb-gain bandwidth.

The measured residual phase noise surpasses earlier results reporting f_{ceo} stabilization via gain modulation by an auxiliary laser [21,23]. In contrast to the results reported in Ref. [20], f_{ceo} stabilization via XGM did not improve the locking performance of our system compared to stabilization via pump-modulation. Additional studies involving a model of the relevant time constants determining the locking bandwidths will need to be carried out to provide further insights into the differences between our results and earlier works reporting a major locking bandwidth extension via XGM [24,25].

4. Conclusion

In summary, we have compared two low-noise CEO frequency stabilization methods. We have studied the XGM method and compared the results with the commonly-used pump-current modulation approach. For XGM, the gain of the all-PM Yb:fiber-based NALM oscillator was modulated via an external CW laser in order to manipulate the intra-cavity power. Tight locking of the CEO frequency was achieved using both pump-modulation and cross-gain modulation with a residual integrated f_{ceo} phase noise (10 Hz to 1 MHz) of 135 mrad and 157 mrad respectively. With the employed Yb:fiber-based NALM oscillator, the XGM approach did not reveal an improved locking performance.

Funding. Deutsches Elektronen-Synchrotron; Austrian Science Fund (M2561-N36); Swiss Bridge Foundation (20B1-1_175199); GSI Helmholtzzentrum für Schwerionenforschung.

Disclosures. The authors declare no conflicts of interest.

OSA CONTINUUM

Data availability. Data underlying the results presented in this paper are not publicly available at this time but may be obtained from the authors upon reasonable request.

References

1. T. Fortier and E. Baumann, "20 years of developments in optical frequency comb technology and applications," Commun. Phys. **2**(1), 153 (2019).
2. S. A. Diddams, "The evolving optical frequency comb [Invited]," J. Opt. Soc. Am. B **27**(11), B51–B62 (2010).
3. N. Picqué and T. W. Hänsch, "Frequency comb spectroscopy," Nat. Photonics **13**(3), 146–157 (2019).
4. T. Udem, J. Reichert, R. Holzwarth, and T. W. Hänsch, "Absolute Optical Frequency Measurement of the Cesium D1 Line with a Mode-Locked Laser," Phys. Rev. Lett. **82**(18), 3568–3571 (1999).
5. N. Newbury, "Searching for applications with a fine-tooth comb," Nat. Photonics **5**(4), 186–188 (2011).
6. M. Hofer, M. E. Fermann, F. Haberl, M. H. Ober, and A. J. Schmidt, "Mode locking with cross-phase and self-phase modulation," Opt. Lett. **16**(7), 502–504 (1991).
7. M. E. Fermann, M. J. Andrejco, Y. Silberberg, and M. L. Stock, "Passive mode locking by using nonlinear polarization evolution in a polarization-maintaining erbium-doped fiber," Opt. Lett. **18**(11), 894–896 (1993).
8. U. Keller, K. J. Weingarten, F. X. Kärtner, D. Kopf, B. Braun, I. D. Jung, R. Fluck, C. Hönninger, N. Matuschek, and J. Aus Der Au, "Semiconductor saturable absorber mirrors (SESAM's) for femtosecond to nanosecond pulse generation in solid-state lasers," IEEE J. Sel. Top. Quantum Electron. **2**(3), 435–453 (1996).
9. D. Popa, Z. Sun, F. Torrisi, T. Hasan, F. Wang, and A. C. Ferrari, "Sub 200 fs pulse generation from a graphene mode-locked fiber laser," Appl. Phys. Lett. **97**(20), 203106 (2010).
10. Y.-W. Song, S. Yamashita, C. S. Goh, and S. Y. Set, "Carbon nanotube mode lockers with enhanced nonlinearity via evanescent field interaction in D-shaped fibers," Opt. Lett. **32**(2), 148–150 (2007).
11. J. Szczepanek, T. Kardaś, C. Radzewicz, and Y. Stepanenko, "Ultrafast laser mode-locked using nonlinear polarization evolution in polarization maintaining fibers," Opt. Lett. **42**(3), 575–578 (2017).
12. M. Lezius, T. Wilken, C. Deutsch, M. Giunta, O. Mandel, A. Thaller, V. Schkolnik, M. Schiemangk, A. Dinkelaker, A. Kohfeldt, A. Wicht, M. Krutzik, A. Peters, O. Hellmig, H. Duncker, K. Sengstock, P. Windpassinger, K. Lampmann, T. Hülsing, T. W. Hänsch, and R. Holzwarth, "Space-borne frequency comb metrology," Optica **3**(12), 1381–1387 (2016).
13. W. Hänsel, H. Hoogland, M. Giunta, S. Schmid, T. Steinmetz, R. Doubek, P. Mayer, S. Dobner, C. Cleff, M. Fischer, and R. Holzwarth, "All polarization-maintaining fiber laser architecture for robust femtosecond pulse generation," Appl. Phys. B **123**(1), 41 (2017).
14. N. Kuse, J. Jiang, C.-C. Lee, T. R. Schibli, and M. E. Fermann, "All polarization-maintaining Er fiber-based optical frequency combs with nonlinear amplifying loop mirror," Opt. Express **24**(3), 3095–3102 (2016).
15. Y. Li, N. Kuse, A. Rolland, Y. Stepanenko, C. Radzewicz, and M. E. Fermann, "Low noise, self-referenced all polarization maintaining Ytterbium fiber laser frequency comb," Opt. Express **25**(15), 18017–18023 (2017).
16. A. Mayer, W. Grosinger, J. Fellinger, G. Winkler, L. Perner, S. Droste, S. Salman, C. Li, C. Heyl, I. Hartl, and O. Heckl, "Flexible all-PM NALM Yb:fiber laser design for frequency comb applications: operation regimes and their noise properties," Opt. Express **28**(13), 18946–18968 (2020).
17. H. Telle, G. Steinmeyer, A. Dunlop, J. Stenger, D. H. Sutter, and U. Keller, "Carrier-envelope offset phase control: A novel concept for absolute optical frequency measurement and ultrashort pulse generation," Appl. Phys. B **69**(4), 327–332 (1999).
18. B. Washburn, W. Swann, and N. Newbury, "Response dynamics of the frequency comb output from a femtosecond fiber laser," Opt. Express **13**(26), 10622–10633 (2005).
19. C.-C. Lee, C. Mohr, J. Bethge, S. Suzuki, M. E. Fermann, I. Hartl, and T. R. Schibli, "Frequency comb stabilization with bandwidth beyond the limit of gain lifetime by an intracavity graphene electro-optic modulator," Opt. Lett. **37**(15), 3084–3086 (2012).
20. W. Hänsel, M. Giunta, M. Lezius, M. Fischer, and R. Holzwarth, "Electro-optic modulator for rapid control of the carrier-envelope offset frequency," in *Conference on Lasers and Electro-Optics, OSA Technical Digest (online)* (Optical Society of America, 2017).
21. M. Hoffmann, S. Schilt, and T. Südmeyer, "CEO stabilization of a femtosecond laser using a SESAM as fast opto-optical modulator," Opt. Express **21**(24), 30054–30064 (2013).
22. O. Pronin, M. Seidel, F. Lücking, J. Brons, E. Fedulova, M. Trubetskov, V. Pervak, A. Apolonski, T. Udem, and F. Krausz, ""High-power multi-megahertz source of waveform-stabilized few-cycle light," Nat. Commun. **6**(1), 6988 (2015).
23. S. Hakobyan, V. J. Wittwer, K. Gürel, A. S. Mayer, S. Schilt, and T. Südmeyer, "Carrier-envelope offset stabilization of a GHz repetition rate femtosecond laser using opto-optical modulation of a SESAM," Opt. Lett. **42**(22), 4651–4654 (2017).
24. L. Karlen, G. Buchs, E. Portuondo-Campa, and S. Lecomte, "Efficient carrier-envelope offset frequency stabilization through gain modulation via stimulated emission," Opt. Lett. **41**(2), 376–379 (2016).
25. K. Gürel, S. Schilt, and T. Südmeyer, "Carrier-Envelope Offset Frequency Stabilization of a Fiber Laser by Cross Gain Modulation," IEEE Photonics J. **10**(2), 1–6 (2018).

OSA CONTINUUM

26. J. R. C. Andrade, N. Modsching, A. Tajalli, C. M. Dietrich, S. Kleinert, F. Placzek, B. Kreipe, S. Schilt, V. J. Wittwer, T. Südmeyer, and U. Morgner, "Carrier-Envelope Offset Frequency Stabilization of a Thin-Disk Laser Oscillator via Depletion Modulation," IEEE Photonics J. **12**(2), 1–9 (2020).
27. M. Seidel, J. Brons, F. Lücking, V. Pervak, A. Apolonski, T. Udem, and O. Pronin, "Carrier-envelope-phase stabilization via dual wavelength pumping," Opt. Lett. **41**(8), 1853–1856 (2016).
28. M. E. Fermann, F. Haberl, M. Hofer, and H. Hochreiter, "Nonlinear amplifying loop mirror," Opt. Lett. **15**(13), 752 (1990).
29. Hong Lin, D. K. Donald, and W. V. Sorin, "Optimizing polarization states in a figure-8 laser using a nonreciprocal phase shifter," J. Lightwave Technol. **12**(7), 1121–1128 (1994).
30. L. Dong, B. K. Thomas, and L. Fu, "Highly nonlinear silica suspended core fibers," Opt. Express **16**(21), 16423–16430 (2008).